Available online at www.sciencedirect.com

ScienceDirect

Energy Procedia 81 (2015) 1077 – 1089

Energy Procedia

69th Conference of the Italian Thermal Engineering Association, ATI 2014

Single cylinder internal combustion engine fuelled with H_2NG operating as micro-CHP for residential use: preliminary experimental analysis on energy performances and numerical simulations for LCOE assessment

Livio de Santoli[a], Gianluigi Lo Basso[b], Angelo Albo[b], Daniele Bruschi[b], Benedetto Nastasi[b,]*

[a]*Interdisciplinary Centre for Landscape, Building, Conservation, Environment (CITERA), Sapienza University of Rome, Via Antonio Gramsci, 53, 00197 Rome, Italy*

[b]*Department of Astronautical, Electrical and Energy Engineering (DIAEE), Sapienza University of Rome, Via Eudossiana, 18, 00184 Rome, Italy*

Abstract

The paper presents data resulting by the preliminary experimental campaign performed on a micro CHP (combined heat and power) pre-commercial version (5kW$_{el}$) designed for dwellings. The engine employs the lubricant oil as the jacket coolant to simplify the heat recovery architecture and it was equipped by a condensing heat exchanger as well. The tests have been carried out at rated and partial load up to 2.9 kW$_{el}$ (59% of rated load) in condensing mode, fuelling the NG engine with hydrogen percentages equal to 0% vol. and 15% vol. In order to evaluate the CHP energy performance, the analysis was conducted for 160 h, using an alkaline electrolyser for hydrogen production, a static heat meter and two mass flow meters for both hydrogen and NG. The aim of this paper is to illustrate how the use of the hydrogen enrichment in a micro CHP plant, based on ICE technology, represents a foreseeable bridge solution to the forthcoming SOFC deployment.

Peer-review under responsibility of the Scientific Committee of ATI 2014

Keywords: Smart Grid; Hybrid System; Micro CHP; Internal Combustion Engine; H2NG; Renewable Hydrogen; LCOE; residential building applications.

* Corresponding author. Tel.: +39-06-4991-9172; fax: +39-06-4991-9171 .
E-mail address: benedetto.nastasi@outlook.com

Peer-review under responsibility of the Scientific Committee of ATI 2014
doi:10.1016/j.egypro.2015.12.130

1. Introduction

The hydrogen addition to gaseous or liquid fuels offers good environmental and energy performances as it was well proven in the last decade[1-8]. In fact, owing to a higher H/C ratio of the hydrogen enriched mixtures and to a faster laminar speed burning[9], CO and CO_2 emissions can be reduced largely, while lower NO_x concentrations are achievable in ultra-lean combustion conditions (i.e. for H_2NG the relative equivalence ratio ranges in $1.54 < \lambda < 2$) [10]. As a consequence the NG enrichment was become attractive for automotive and for static power generation applications such as CHP for buildings and small scale production processes[11].

Since the residential sector as well as the historical buildings represent a high percentage of national energy consumption, they has recently become attractive targets for the CHP and µCHP system integration [12].

Moreover, the designation of ‘‘micro’’ is derived from the appliances power producing capability, where micro is any system under 20 kW_{el} [13].

Currently, several conversion technologies such as PEMFC and SOFC, MGT, Stirling engine, MRC and ICE are available on the market as prototype, pre-commercial and commercial versions related to systems size.

PEMFC technology, working at operating conditions characterized by atmospheric pressure and low temperature, has great advantages in terms of construction and plant engineering[14]. Nevertheless the main drawbacks consist of a limited membrane lifetime and a required high hydrogen purity degree (99.995 %vol. at least).

SOFCs are one of the most promising configurations of fuel cells because of its high energy efficiency (e.g. first law efficiency ranges from 85% up to 102%), fuel flexibility, modularity, and the absence of corrosive liquids [15].

However, obstacles encountered for SOFCs deployment are the great unit specific costs and a remarkable decreasing lifetime due to a discontinuous operation.

Internal combustion engines are the most well-established technology for small and micro CHP applications especially in terms of reliability[16]. Referring to available commercial systems designed for dwellings, the electrical efficiency ranges from 20% to 27%, with a potential CHP first law efficiency up to 95% depending on end-user set point temperature. Even though ICE behavior is well known and further developments are limited, investigations on engine fuelling with alternative eco-fuels could be interesting.

In this paper a preliminary experimental analysis on condensing µCHP fuelled with H_2NG@15% vol. was presented. Specifically, the hydrogen enrichment effects on both electrical and heat recovery efficiencies were investigated. Finally, numerical simulations were performed in order to assess the LCOE along with a sensitivity analysis with varying the H_2NG and H_2 costs, which plays a key role for spreading out all of H_2-based technologies.

Nomenclature

AEEG	Authority for electric energy and gas	MGT	Micro gas turbine
C_{ann}	annualized cost [€/yr]	MRC	Micro Rankine cycle
CAC	Carbon avoidance cost[€/kg]	N	Investment lifetime
µCHP	Micro combined heat and power	NG	Natural gas
H_2NG	Hydrogen enriched natural gas blend	NPC	Net present cost [€]
HRR	Heat recovery ratio	NPV	Net present value [€]
i	Interest rate for actualization [1.53%]	PEMFC	Proton exchange membrane fuel cell
ICE	Internal combustion engine	SOFC	Solide oxide fuel cell
LCOE	Levelized cost of electricity [€/kWh]	VOP	Blend volumetric overprice [€/Nm^3]
LHV	Lower heating value [kJ/Nm^3]	VSD	Variable speed drive

2. Appliance description and methodology

The preliminary experimental campaign was carried out on a single cylinder Natural Gas engine based on Otto cycle, equipped with a 3-way catalyst and Lambda probe, designed for dwelling applications. The engine control unit allows to modulate the electrical power output acting on the shaft rotational speed. The electrical generator is connected to a static frequency converter in order to assure 50 Hz for all of partial load conditions. Moreover, the whole electrical conversion system is characterized by an efficiency close to 94 %. Table 1 reports the engine technical characteristics and the operating temperature range for the end-user connection. The same oil for moving parts lubrication was employed as engine coolant, recovering heat from electrical generator and cylinder jacket as well. An oil/water plane heat exchanger provides the water pre-heating of end-user hydraulic loop. Finally, the hot water flows through a small shell tube gas/liquid heat exchanger which is able to condense out an exhaust water content fraction allowing the sensible and latent heat recovery. Figure 1 shows clearly the heat recovery architecture and temperature probes layout. In addition, a remote monitoring system allows to register the oil, water and exhaust gas temperature along with the engine water inlet and outlet ones. Thus, in order to measure the μCHP thermal energy production, a heat meter on the end- user loop side was installed. The experimental tests regarded the μCHP energy characterization, in terms of electrical and thermal efficiencies assessment with varying the rotational speed, when NG and H_2NG blend have been applied alternatively as fuels. In order to assure the required Methane Number (higher than 80), a hydrogen enriched natural gas mixture with 15% vol. of H_2 was used.

All of measurements were registered referring to condensing conditions, once the engine water inlet temperature has been fixed equal to 35°C. In order to keep under control that temperature, an air cooled exchanger equipped with a VSD on its fan was inserted into the hydraulic loop. The measurements were carried out over one month, running the μCHP for 160 operating hours. In detail, 80 operating hours for each fuel were dedicated to the engine testing at rated and partial load. Thus, five power set point were defined in order to register 320 points globally for each fuel, since the data sampling frequency was set to 15 minutes.

Table 1. μCHP Data sheet.

μCHP Engine Characteristics	
Displacement	499 cm^3
Number of cylinders	1
Cycle	Four strokes
Compression Ratio	10
Rotational Speed	1,500-2,100 rpm
Methane Number Required	> 80
Feeding system	electronic injection
Rated electrical power	0.5 – 5 kW
Rated thermal power	5 – 15 kW
Thermal power from fuel	19.2 kW
Electrical Efficiency	26 %
Max heat recovery efficiency	76 %
Max First law efficiency	102 %
Max outlet temperature	70 °C
Max/min inlet temperature	60/25 °C
Water Flow rate	670 liters/h
Oil tank volume	25 liters

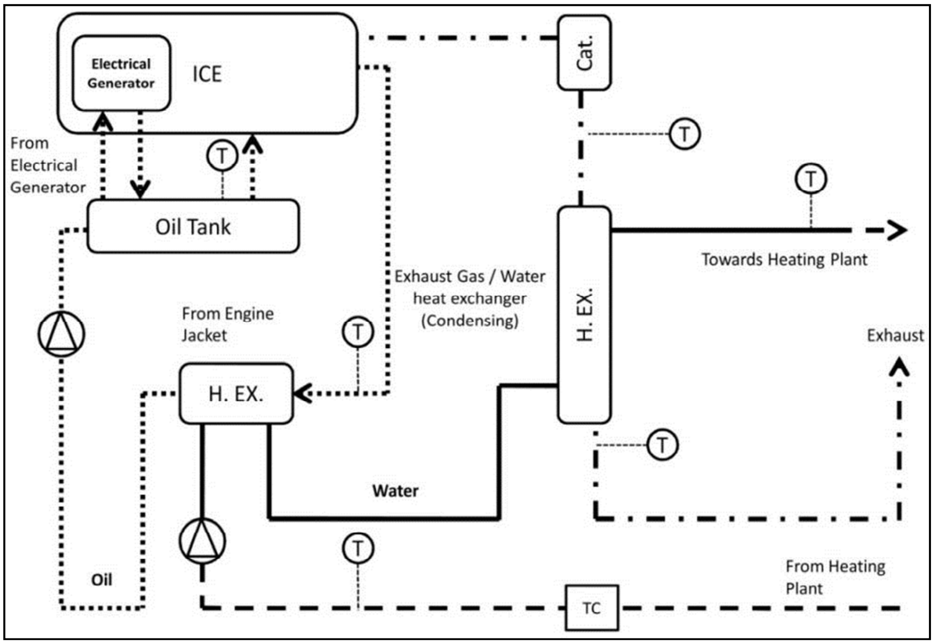

Fig.1 µCHP heat recovery architecture and temperature probes location.

3. Results and Discussion

The µCHP prototype, it is able to recover thermal power from lubrication oil, the exhaust gas sensible ($Ps_{ensible}$) and latent heat (P_{latent}) as well. Consequently, the heat balance reads as:

$$P_{th} = P_{oil} + P_{sensible} + P_{latent} = m_w \cdot c_{p,w} \cdot (T_{w,in} - T_{w,out}) \tag{1}$$

Additionally, the heat recovery efficiency (η_Q) and the electrical efficiency (η_{el}) were evaluated, according to the following equations:

$$\eta_Q = \frac{P_{th}}{q_{blend} \cdot LHV_{blend}} \tag{2}$$

$$\eta_{el} = \frac{P_{el}}{q_{blend} \cdot LHV_{blend}} \tag{3}$$

where q_{blend} indicates the blend flow rate, LHV_{blend} represents the blend lower heating value and P_{el} is the electrical power output. For each load conditions η_{el} and η_Q were deduced from data and their trends were plotted on the same chart (see Fig. 2).

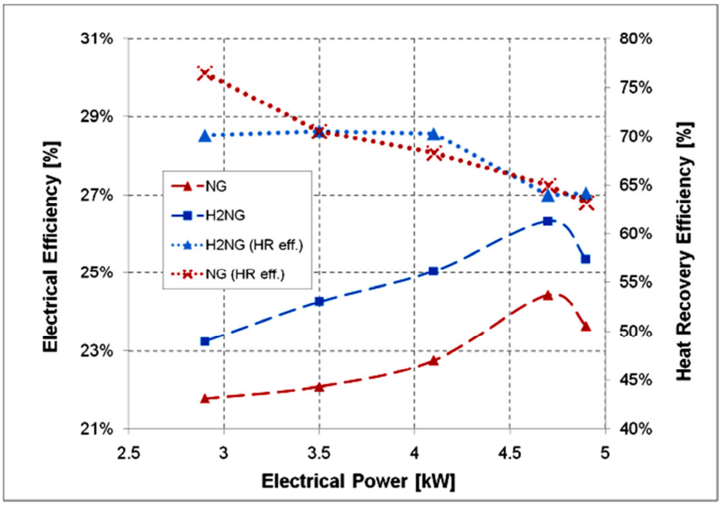

Fig. 2 Electrical and Heat Recovery efficiencies vs. electrical power output, for NG and H_2NG@15% vol. feeding.

It is noteworthy that the engine electrical efficiency increases in all of operating conditions as the hydrogen is blended. Specifically, the maximum gain is equal to 2.276 percentage points as shown in Fig 3 (a). According to the literature [7,11,17] these results show how the H_2NG@15% vol. leads to a higher mechanical performance owing to an improved fuel combustion efficiency along with the enhancement of charge specific heats ratio (γ).

With regard to the heat recovery efficiency, from data emerges a slight reduction when electrical load ranges between 3.5-5 kW_{el}, while the worst value is reached at 2.9 kW_{el}. However, this is mainly due to a lower recoverable thermal power resulting from the higher engine mechanical efficiency which reduces thermodynamic losses.

In addition, heat exchangers operate in off-design conditions caused by the volumetric and temperature derating effects on the exhaust gas side [11,18], even though water condensation partially mitigates this thermal power lessening (see the blue bar chart in Figure 3(a)). The H_2NG lower energy density respect to the NG one implies a greater fuel flow rate for the engine running. In fact, in order to assure the same electrical power output, the CHP control system acts on throttle valve opening and on the injector nozzle cross section by means also of a feedback signal coming from the Lambda probe. In Figure 4 the CHP flow rates for both NG and H_2NG feeding are superimposed highlighting the hydrogen flow rate fraction as well.

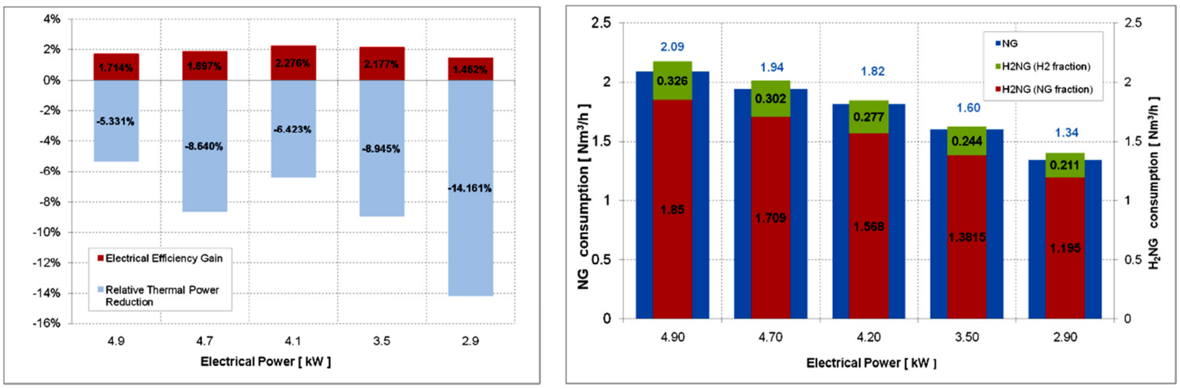

Fig. 3 (a) Electrical efficiency gain and relative thermal power reduction with H2NG@15% vol.; (b) Blends consumption vs. electrical power output.

HRR is a secondary parameter which is useful for the CHP simulation by software applications such as HOMER because this indicator can correlate directly the electrical efficiency with the heat recovery one (see Equation 4).

$$HRR = \frac{P_{th}}{(1-\eta_{el}) \cdot q_{blend} \cdot LHV_{blend}} = \eta_Q \cdot \frac{1}{(1-\eta_{el})} \tag{4}$$

In fact, it represents the waste heat recovery effectiveness. In Figure 5, the CHP thermal power trends as well as those related to HRR were plotted together. It is remarkable that the H_2 enrichment affects positively HRR values with the exception of the lowest partial load case. Notwithstanding, the H_2NG application leads to an enhancement in the averaged HRR over all of load set points (see the blue and yellow dashed lines in Figure 4).

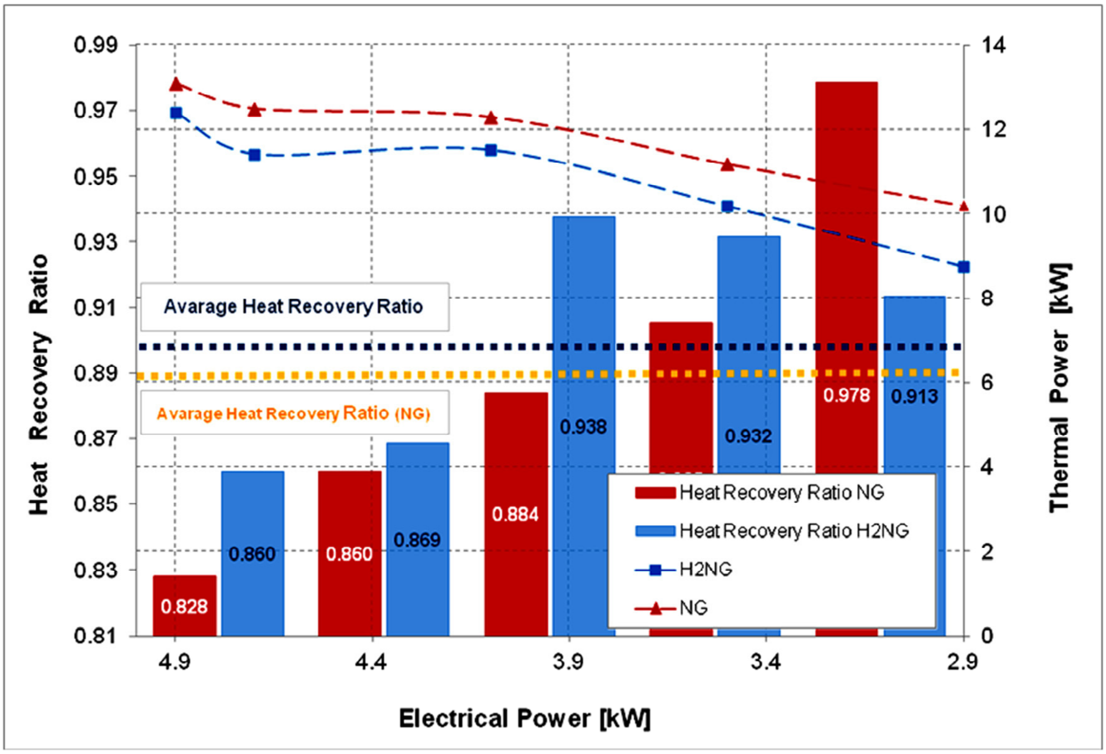

Fig. 4 Thermal power output and HRR vs. electrical power output for NG and H2NG feeding.

3.1. Reference scenarios simulation

In this work two reference energy scenarios were simulated in order to compare immediately the CHP techno-economical performances related to the different gaseous fuels engine feeding.

In fact, the engine was integrated in a computational energy system consisting of two just alike detached houses having 250 m^2 of floor area each one.

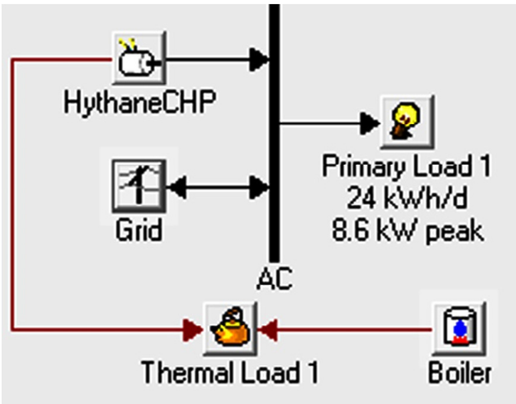

Fig. 5 Energy system: base scenario.

Energy-economic simulations were performed using HOMER 2.81 in order to calculate the system LCOE. The overall electrical and thermal loads were implemented referring to current Italian regulations for new constructions.

In particular, the simulated dwellings belong to C energy class and are located in Rome.

The simulation model layout is depicted in Figure 5, and a methane boiler was implemented as thermal backup. The integral average value over one year period of the electrical and thermal loads were assumed equal to 23.6 kWh/d and 49.3 kWh/d respectively, with the monthly profiles shown in Figures 6 and 7.

Regarding to the electricity purchase price, the Italian time slots were implemented according to AEEG deliberation n°181/06. In addition, the energy sell-back values were based on Italian spot market quotations relative to July 2014 along with NG and H_2NG costs, as reported in Table 2.

For the LCOE determination, the NPV calculation was performed and solved in such a way that for the chosen LCOE value, the project's net present value was zero. Therefore, the LCOE corresponds to the minimum average price at which energy must be sold or to the maximum specific expenditure for energy self-consumption (over the project lifetime) to break even [19]. HOMER simulation tool calculates this parameter by the equation below:

$$LCOE = \frac{C_{ann,Tot} - c_{boiler} \cdot H_{served}}{E_{served}} \qquad (5)$$

Where:

$$C_{ann,Tot} = \frac{i \cdot (1+i)^N}{(1+i)^N - 1} \cdot C_{NPC,Tot} \qquad (6)$$

Table 2. Energy prices overview for base scenarios.

Time Slots	Price [€/kWh]	Sell back [€/kWh]	NG price [€/Nm^3]	H_2NG price [€/Nm^3]
F1	0.300	0.048	-	-
F2	0.300	0.056	0.980	0.979
F3	0.300	0.050	-	-

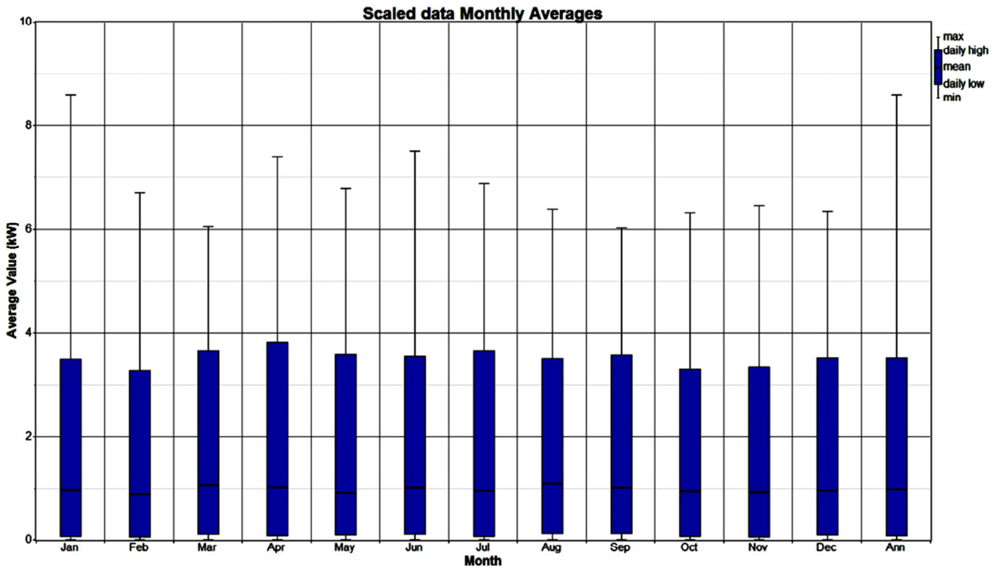

Fig. 6 End users electrical loads.

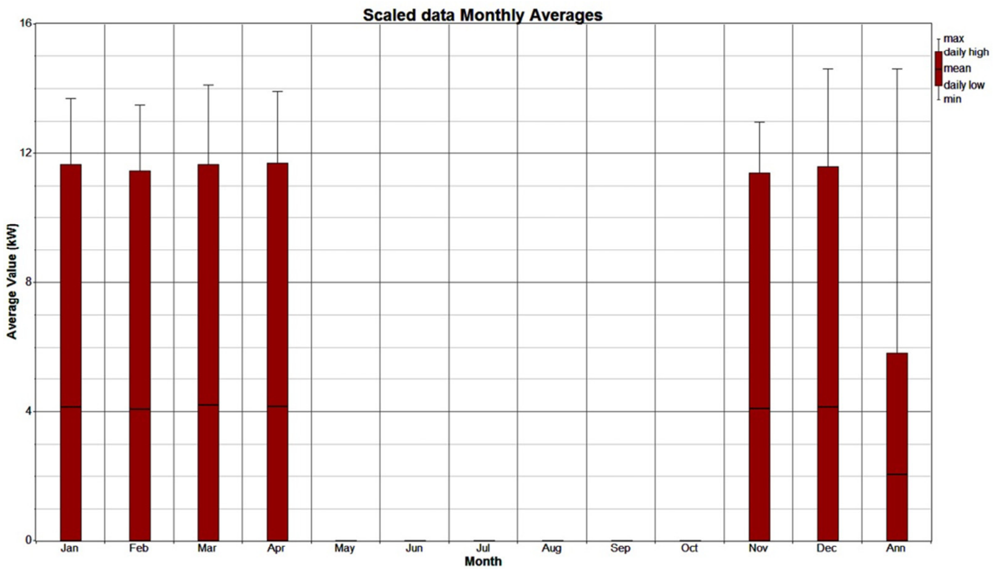

Fig. 7 End users thermal loads.

Equation (6) represents the total annualized costs associated to the energy system:

- c_{boiler} indicates the boiler marginal costs [€/kWh];
- H_{served} is the total thermal load served over one year period [kWh/yr];
- E_{served} is the total electrical load served over one year period.

Regarding to the base scenarios for both H_2NG and NG engine operations, Tables 3 and 4 summarize all of the annualized costs categorized by system components and cost typology. Additionally, the salvage value was computed as well, where it was defined as the value remaining in a component of the power system at the end of the project lifetime. Specifically, HOMER assumes linear components depreciation , meaning that the salvage value of an appliance is directly proportional to its remaining life.

From data emerges the higher overall management costs related to the H_2NG blend application, compared with the NG one, as it was expected. Even though the assumed fuel prices were the same, this result is owing to the lower operating hours and heat production as well. Consequently, that implies a greater value of LCOE, but leads to an interesting annual carbon dioxide emission reduction as reported in Table 5.

Table 3. Annualized costs for H_2NG CHP energy system (base Scenario).

Component	Capital [€/yr]	Replacement [€/yr]	O&M [€/yr]	Fuel [€/yr]	Salvage [€/yr]	Total [€/yr]
H_2NG CHP	789	351	157	2,642	-245	3,694
Grid	0	0	1,792	0	0	1,792
Boiler	0	0	0	551	0	551
System	789	351	1,948	3,192	-245	6,036

Table 4. Annualized costs for NG CHP energy system (base Scenario).

Component	Capital [€/yr]	Replacement [€/yr]	O&M [€/yr]	Fuel [€/yr]	Salvage [€/yr]	Total [€/yr]
NG CHP	789	354	163	2,633	-229	3,709
Grid	0	0	1,750	0	0	1,750
Boiler	0	0	0	442	0	442
System	789	354	1,912	3,074	-229	5,901

Table 5. Compared CHP operating parameters (base Scenarios).

System	LCOE [€/kWh]	Operating hours [hr/yr]	Fuel Consumption [Nm^3/yr]	Electrical production [kWh/yr]	Heat production [kWh/yr]	$CO_{2\ sys}$ [kg/yr]	$CO_{2\ ,fuel}$ [kg/yr]
NG CHP	0.324	1,959	2,686	5,715	18,617	7,465	5,272.6
H2NG CHP	0.336	1,888	2,697	5,546	16,562	6,987	4,499.9

3.2. Sensitivity analysis

In order to complete this study a sensitivity analysis on the energy system LCOE and carbon avoidance cost was performed. H_2NG blend purchase price, CHP capital expenditure and HRR were defined as the dominating factors affecting the final cost of electricity which matches all of technical and economic constraints for the implemented energy scenario. Specifically, the NG price was assumed equal to 0.98 €/Nm^3 representing the average supply cost on Italian market for a common domestic end-user. Furthermore, all of tariff components such as NG distribution, storage, retail, and energy burdens, as well as excises and VAT were included.

As regards to the hydrogen prices, LCOHs associated to the renewable hydrogen production system integrated in a larger Smart Grid were assumed from literature [20].

Given that, the blend price can be evaluated by the following equation, once the hydrogen fraction for the NG enrichment has been decided:

$$C_{H2NG} = C_{NG} \cdot (1 - f_{H2}) + C_{H2} \cdot f_{H2} \quad (7)$$

Where:

- C_{H2NG} indicates the H_2NG blend price expressed by €/Nm^3;
- C_{NG} is the total thermal load served over one year period [kWh/yr];
- C_{H2} is the levelized cost of renewable hydrogen expressed by €/Nm^3;
- f_{H2} is the hydrogen content by volume.

As a consequence, the volumetric H_2NG over price can be calculated by Equation 8:

$$VOP = C_{H2NG} - C_{NG} = (C_{H2} - C_{NG}) \cdot f_{H2} \tag{8}$$

Referring to the present case study, Figure 8 depicts the H_2NG@15% prices with varying the renewable hydrogen cost considered for these simulations. It is noteworthy, when the renewable hydrogen production cost is lower than 0.9762 €/Nm^3 a volumetric saving for fuel supply is achievable, allowing to a partial trade-off related to the lower H_2NG density and its specific energy by volume.

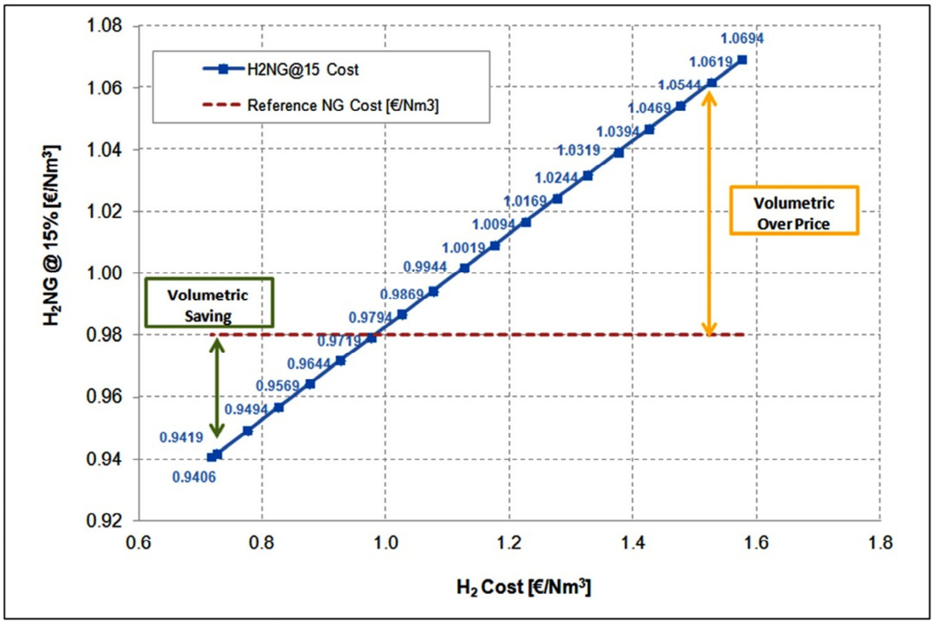

Fig. 8 H_2NG@15% price with varying the hydrogen cost.

In order to compare properly the economic effects, related to the H_2NG purchase price changes, on LCOE, the HRR average value for CHP (i.e. equal to 0.9) was considered in each simulation sub scenarios. In Table 6 all of technical and economic data have been reported in a systemic overview. In detail, increasing the H_2NG price from the minimum value equal to 0.941 €/Nm^3 up to 1.069 €/Nm^3 the LCOE differences (ΔLCOE) are always higher than zero and correspond to +0.003 €/kWh and +0.032 €/kWh respectively.

This is due to the fact that the larger is the blend price, the larger are marginal and fixed costs of system energy production. Moreover owing to the HOMER's optimization criteria the CHP operating hours tend to shrink slightly penalizing the system capacity factor. Finally, from Figure 9 it is possible to asses immediately the overall or single influence of selected parameters on the final LCOE value. Furthermore, it is important to point out that the best estimated scenario configuration was obtained by a HRR equal to 0.94 along with the lowest simulated blend price.

In these conditions the best LCOE value equates the NG case one (i.e. 0.324 €/kWh).

Table 6. H_2NG CHP operating parameters summary resulting from sensitivity analysis.

H_2NG price [€/Nm^3]	H_2 price [€/Nm^3]	Operating hours [hr/yr]	Blend consumption [Nm^3/yr]	Electrical production [kWh/yr]	Heat production [kWh/yr]	Generation fixed cost [€/h]	Energy marginal cost [€/kWh]	ΔLCOE [€/kWh]
0.941	0.7262	1,936	2,765	5,685	16,979	0,698	0.335	+0.003
0.949	0.7762	1930	2,757	5,668	16,927	0.701	0.338	+0.005
0.957	0.8262	1,923	2,747	5,647	16,866	0.704	0.341	+0.006
0.979	0.9762	1,888	2,697	5,546	16,562	0.713	0.349	+0.012
1.054	1.4762	1,828	2,612	5,372	16,040	0.741	0.375	+0.028
1.062	1.5262	1,823	2,605	5,357	15,995	0.744	0.378	+0.030
1.069	1.5762	1,819	2,599	5,345	15,959	0.747	0.381	+0.032

On an environmental point of view, it was interesting to estimate the associated carbon dioxide avoidance costs (CAC) resulting from hydrogen application as a carbon-free fuel additive within the µCHP. Firstly, the CAC which is strictly connected to the blend use for engine feeding were calculated according to Equation 9:

$$C_{CO2(CHP)} = \frac{C_{ann,fuel(H2NG)} - C_{ann,fuel(NG)}}{\Delta CO_{2,fuel}} \quad (9)$$

Secondly, the CAC related to the overall energy system were calculated by Equation 10:

$$C_{CO2(Sys)} = \frac{C_{ann,tot(H2NG)} - C_{ann,tot(NG)}}{\Delta CO_{2,sys}} \quad (10)$$

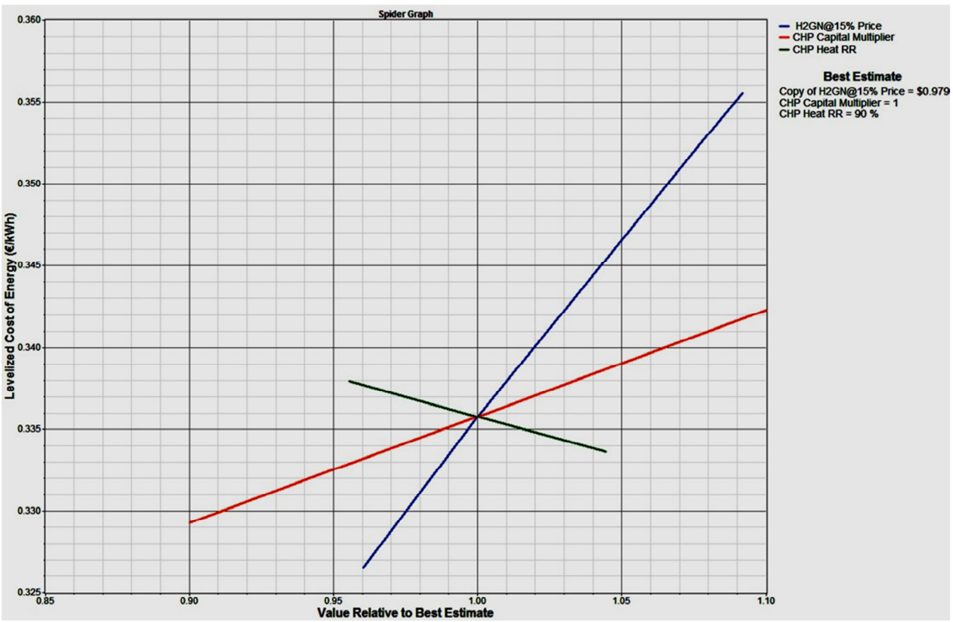

Fig. 9 Graphical summary of sensitivity analysis results: LCOE variations referred to the H_2NG base scenario.

In Table 8 the overall CAC values are reported and an overcharge was registered for all H_2NG price scenarios. Lastly, referring to the best estimated scenario, it leads to -0.0268 €/kg for the first indicator and to 0.0103 €/kg for the second one.

Table 7. H_2NG CHP associated carbon avoidance cost.

H_2NG price [€/Nm^3]	H_2 price [€/Nm^3]	$CO_{2\ sys}$ [kg/yr]	$\Delta CO_{2,\ sys}$ [kg/yr]	$CO_{2\ blend}$ [kg/yr]	$\Delta CO_{2,\ fuel}$ [kg/yr]	Fuel annualized cost for CHP [€/yr]	Carbon avoidance cost [€/kg]
0.941	0.7262	6,949	-516	4,613.35	-659.25	2,601	-0.0485
0.949	0.7762	6,954	-511	4,599.99	-672.61	2,617	-0.0237
0.957	0.8262	6,959	-506	4,583.31	-689.29	2,628	-0.0072
0.979	0.9762	6,987	-468	4,499,90	-772.7	2,642	+0.0116
1.054	1.4762	7,034	-431	4,358.06	-914.54	2,754	+0.1323
1.062	1.5262	7,039	-426	4,346.39	-926.21	2,766	+0.1436
1.069	1.5762	7,042	-423	4,336.38	-936.22	2,780	+0.1570

Table 8. H_2NG CHP associated carbon avoidance cost in the whole energy system.

H_2NG price [€/Nm^3]	H_2 price [€/Nm^3]	Grid purchase [€/yr]	NG cost for boiler [€/yr]	System annualized cost [€/yr]	$\Delta C_{ann,\ sys}$ [€/yr]	System carbon avoidance cost [€/kg]
0.941	0.7262	1,754	506	5,930	+29	+0.0562
0.949	0.7762	1,759	512	5,955	+54	+0.1056
0.957	0.8262	1,764	518	5,975	+74	+0.1462
0.979	0.9762	1,792	551	6,036	+135	+0.2884
1.054	1.4762	1,843	606	6,234	+333	+0.7726
1.062	1.5262	1,848	611	6,254	+353	+0.8286
1.069	1.5762	1,852	615	6,274	+373	+0.8818

Tables 7 and 8 report all of quantities which were required for these two indicators calculation. Referring to the CHP engine operation only, it is notable (see Table 7) that the CAC enhances in a step-wise fashion as the blend price increases. Additionally, when H_2NG price is lower than 0.979 €/Nm^3 the first indicator has a negative value implying an economical saving for this decarbonization process.

Indeed, beyond that price threshold an overcharge has to be paid for carbon reduction. When the whole energy system is considered, all of contributes to carbon emission related to electricity purchase from the grid and to the backup boiler have to be accounted for, as well as their annualized costs.

4. Conclusions

The data analysis shows that with a hydrogen content close to 15% vol. meaningful electrical efficiency gains are achievable. Yet, the heat recovery efficiency is penalized for all load conditions, increasing the CHP power to heat ratio and First Law efficiency as well. Optimizing the engine heat recovery system when it is fuelled with H_2NG, the LCOE parity with NG running can be attained along with a CAC close to zero.

References

[1] Dimopoulos P, Rechsteiner C, Soltic P, Laemmle C, Boulouchos K. Increase of passenger car engine efficiency with low engine-out emissions using hydrogenenatural gas mixtures: a thermodynamic analysis. Int J Hydrogen Energy 2007;32(14):3073-83.

[2] Bysveen M. Engine characteristics of emissions and performance using mixtures of natural gas and hydrogen. Energy 2007;32(4):482-9.

[3] Dimopoulos P, Bach C, Soltic P, Boulouchos K. Hydrogen-natural gas blends fuelling passenger car engines: combustion, emissions and well-to-wheels assessment. Int J Hydrogen Energy 2008;33(23):7224-36.

[4] Perini F, Paltrinieri F, Mattarelli E. A quasi-dimensional combustion model for performance and emissions of SI engines running on hydrogen-methane blends. Int J Hydrogen Energy 2010;35(10):4687-701.

[5] Fanhua M, Mingyue W, Long J, Jiao D, Renzhe C, Nashay N, et al. Performance and emission characteristics of a turbocharged spark-ignition hydrogenenriched compressed natural gas engine under wide open throttle operating conditions. Int J Hydrogen Energy 2010;35(22):12502-9.

[6] Park J, Cha H, Song S, Chun KM. A numerical study of a methane-fuelled gas engine generator with addition of hydrogen using cycle simulation and DOE method. Int J Hydrogen Energy 2011;36(8):5153-62.

[7] Park C, Kim C, Choi Y, Won S, Moriyoshi Y. The influences of hydrogen on the performance and emission characteristics of a heavy duty natural gas engine. Int J Hydrogen Energy 2011;36(5):3739-45.

[8] Çeper BA. Use of hydrogen-methane blends in internal combustion engines. In: Minic D, editor. Hydrogen energy challenges and perspectives. Rijeka, Croatia: InTech; 2012, ISBN 978-953-51-0812-2; 2012.

[9] Ilbas, M., Crayford, A., Yilmaz, I., Bowen, P. & Syred, N. Laminar-burning velocities of hydrogen-air and hydrogen-methane-air mixtures: An experimental study. Int J Hydrogen Energy 2006; 31: 1768–1779.

[10] Ma F., Ding S., Wang Y., Wang Yefu, Wang J., Zhao S. Study on combustion behaviors and cycle-by-cycle variations in a turbocharged lean burn natural gas S.I. engine with hydrogen enrichment. 2008 Int J Hydrogen Energy; 33: 7245-7255.

[11] de Santoli L, Lo Basso G, Bruschi D. Energy characterization of CHP fuelled with hydrogen enriched natural gas blends. Energy 2013;60:13-22.

[12] Salata F. De Lieto Vollaro A, de Lieto Vollaro R. A case study of technical and economic comparison among energy production systems in a complex of historic buildings in Rome. Energy Procedia 2014;45:482-491.

[13] Bianchi M, De Pascale A,. Spina PR. Guidelines for residential micro-CHP systems design. Applied Energy 2012;97:673-685.

[14] Barelli L, Bidini G, Gallorini F, Ottaviano A. An energetic–exergetic comparison between PEMFC and SOFC-based micro-CHP systems. Int J Hydrogen Energy 2011;36(4):3206–3214.

[15] Zhao Y, Xia C, Jia L, Wang Z, Li H, Yu J, Li Y. Recent progress on solid oxide fuel cell: Lowering temperature and utilizing non-hydrogen fuels. Int J Hydrogen Energy 2013;38(36):16498–16517.

[16] Peruzzi L, Salata F, de Lieto Vollaro A, de Lieto Vollaro R. The reliability of technological systems with high energy efficiency in residential buildings. Energy Build 2014;68:19-24.

[17] de Santoli L, Lo Basso G, Bruschi D. Preliminary Experimental Analysis of a CHP Hydromethane System. Journal of Energy and Power Engineering 2013;7:1681-1690.

[18] de Santoli L, Lo Basso G, Bruschi D. Hybrid system with an integrated CHP plant fuelled by H_2NG blends: theoretical energy-environmental analysis and foreseeable optimizations. Energy Build 2014;71:88-94.

[19] Kornbluth K, Greenwood J, Jordan E, McCaffrey Z, Erickson P. A. Economic feasibility of hydrogen enrichment for reducing NOx emissions from landfill gas powergeneration alternatives:A comparison of the levelized cost of electricity with present strategies. Energy Policy 2012;41:333-339.

[20] de Santoli L, Lo Basso G, Bruschi D. A small scale H_2NG production plant in Italy: Techno-economic feasibility analysis and costs associated with carbon avoidance. Int J Hydrogen Energy 2014;39(12):6497–6517.